Anomaly detection of motion capture data based on the autoencoder approach

Piotr Hasiec[1] *, Adam Świtoński[1]**[0000−0003−4836−6418], Henryk Josiński[1][0000−0003−0196−7777], and Konrad Wojciechowski[2][0000−0003−4679−2667]

[1] Department of Computer Graphics, Vision and Digital Systems, Silesian University of Technology, ul. Akademicka 16, 44-100 Gliwice, Poland
adam.switonski@polsl.pl, henryk.josinski@polsl.pl

[2] Polish-Japanese Academy of Information Technology, Aleja Legionów 2, 41-902 Bytom, Poland
konrad.wojciechowski@pja.edu.pl

Abstract. Anomalies of gait sequences are detected on the basis of an autoencoder strategy in which input data are reconstructed from their embeddings. The denoising dense low-dimensional and sparse high-dimensional autoencoders are applied for segments of time series representing 3D rotations of the skeletal body parts. The outliers – misreconstructed time segments – are determined and classified as abnormal gait fragments. In the validation stage, motion capture data registered in the virtual reality of the Human Dynamics and Multimodal Interaction Laboratory of the Polish-Japanese Academy of Information Technology equipped with Motek CAREN Extended hardware and software are used. The scenarios with audio and visual stimuli are prepared to enforce anomalies during a walk. The acquired data are labeled by a human, which results in the visible and invisible anomalies extracted. The neural network representing the autoencoder is trained using anomaly-free data and validated by the complete ones. AP (Average Precision) and ROC-AUC (Receiver Operating Characteristic – Area Under Curve) measures are calculated to assess detection performance. The influences of the number of neurons of the hidden layer, the length of the analyzed time segments and the variance of injected Gaussian noise are investigated. The obtained results, with AP = 0.46 and ROC-AUC = 0.71, are promising.

Keywords: anomaly detection, motion capture, gait analysis, autoencoder, CAREN Extended, neural networks

1 Introduction

The motion capture acquisition gives precise measurements of human movements. The attached markers on the anatomically significant body points are

* P. Hasiec is a student of computer science at the Silesian University of Technology
** Corresponding author

ICCS Camera Ready Version 2023
To cite this paper please use the final published version:
DOI: 10.1007/978-3-031-36021-3_59

tracked by the calibrated multicamera system. Thus, their 3D positions in the global system for the subsequent time instants are reconstructed. As a result, the relative orientations between adjacent skeletal segments can be established. They are represented by a 3D rotation of joints connecting segments. Motion capture data have a form of multivariate time series of successive poses described by Euler angles or unit quaternions. There are plenty of applications for motion capture registration. Among others, it was successfully used in the diagnosis of movements abnormalities related to selected diseases [16], human gait identification [23], kinematic analysis of body movements performed by sport athlets [6], daily activities classification [2] or assessments of personal nonverbal interactions [5].

Anomalies can be defined as data instances that significantly deviate from the majority of them [18] or patterns that do not conform to expected typical behavior [8]. Their detection is a semi-supervised classification problem. It means that the training set contains only normal data. There are no anomaly instances; their nature is unknown. The problem is similar to the determination of outliers (this term is further used interchangeably with anomaly), the values which are very different from all the others. Anomaly detection is broadly conducted for numerous types of data. It was applied in the detection of host-based and network-based intrusion, banking systems and mobile phone frauds, monitoring of medical and public health, unmasking industrial damages as well as text and sensor data [18].

Although the problem of anomaly detection is extensively studied, there are no publications strictly devoted to gait data and highly precise motion capture measurements, which is the subject of the paper. Two variants of autoencoder strategy – denoising dense low-dimensional and sparse high-dimensional – are selected, adapted and successfully validated in human gait anomaly detection. Moreover, the contribution of the paper is related to the innovative collected dataset, with the registration taking place in the virtual reality of the Motek CAREN Extended laboratory.

2 Related work

According to [7], multivariate time sequence anomalies can be categorized as point, subsequence or time series ones. It means that a single time instant – point, the consecutive points in time – subsequence, or entire time series constructed by subset of its variables, that behaves unusually when compared to the other values either locally or globally are detected. The model-based approaches are most commonly used to accomplish the task. They rely on the determination of the expected value and its comparison to the actual one. Depending on the difference, the anomaly is identified or not. There are two major variants – estimation and prediction. In the first one, the expected value is computed on the basis of previous and current time instants, while in the second variant, only previous values are taken. The most simple models are based on baseline statistics such as the median [3], local means and standard deviations [9]. Other ones

ICCS Camera Ready Version 2023
To cite this paper please use the final published version:
DOI: 10.1007/978-3-031-36021-3_59

try to estimate the unlikeness of values, assuming, for instance, that data without outliers have mixed normal distribution [21]. Alternative proposals which analyze the trends of local changes are slope-based. In [22], constraints are established as a maximum and a minimum possible difference between consecutive points and in [24] there is an assumption of insignificant local slope changes.

However, in the estimation approaches of the model-based category, the most broadly applied are the autoencoders [1,10]. They are typically neural networks that learn only the most common and significant features, which can be realized by determining low-dimensional embeddings in a hidden layer or sparse connections between neurons. Due to the training being based on anomaly-free data, the anomalies correspond to non-representative features, which means that their precise reconstruction fails. To take into account temporal dependencies, overlapping sliding windows are processed as in [14].

In the prediction approaches, an auto-regressive moving average (ARMA) model [25], convolutional neural networks (CNN) [17] or long-short memory (LSTM) units [11] are used.

Another category of anomaly detection techniques are density-based methods [7]. They assume that in every surrounding of analyzed time instant, there are only a few outliers. Thus, the distances between a given time instant and the ones in its surrounding are calculated. Further, the number of instances with dissimilarities greater than specified threshold value is counted and decides about the anomaly identification.

As regards the methods strictly devoted to subsequence anomalies, discord approaches [13] are quite common. They determine the most unusual subseries by comparing dissimilarities between every pair of subsequences. For time series anomalies, dimensionality reduction techniques can be employed as for instance Principal Component Analysis [12]. In other common variants clustering as k-means algorithm [20] or agglomerative hierarchical one [15] is carried out. In [4] additionally Dynamic Time Warping is utilized to align and compare complete time series.

3 Method

Due to the pioneering application of anomaly detection to gait motion capture data, the baseline and most broadly used approach is selected – the autoencoder strategy. Its structure consists of three main components – encoder, decoder and hidden layer. Input data are reconstructed on the basis of their representation by the hidden layer, typically with lower dimensionality as visualized in Fig. 1. If E and D are encoder and decoder transfer functions to and from the hidden layer, respectively, x and x' denote input and output, the working of the autoencoder is described by the following formula:

$$x' = D(E(x)) \tag{1}$$

It is assumed that normal data are highly correlated and can be represented by low-dimensional embeddings of the hidden layer from which efficient reconstruction is feasible. In the training stage, anomaly-free data are used to establish

ICCS Camera Ready Version 2023
To cite this paper please use the final published version:
DOI: 10.1007/978-3-031-36021-3_59

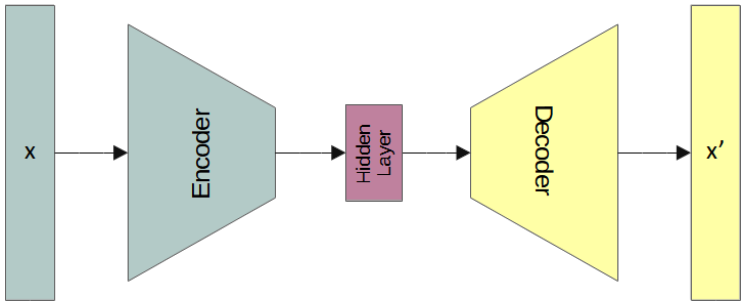

Fig. 1. Autoencoder strategy.

the encoder and decoder workings. Finally, using selected metrics, for instance, Euclidean one, the reconstruction error rE is computed to identify outliers:

$$rE = \|x' - x\| \tag{2}$$

However, the problem of thresholding the rE value on the basis of which anomalies are recognized is not a trivial task. If the normal distribution of the reconstruction error for typical data is naively assumed, the estimated average value increased by two or three standard deviations may be taken. In another possible variant, percentiles of the rE distribution can be used.

Two neural network architectures are chosen for the autoencoder implementation. Primarily, it is a dense low-dimensional variant visualized in Fig. 2a with fewer neurons of the hidden layer than a number of input values. Thus, it works in the standard previously described way – low-dimensional embeddings are determined and reconstruction of the input data is carried out. The second chosen architecture is a sparse high-dimensional network (Fig. 2b) with a greater number of neurons of the hidden layer. To avoid just a simple copy of the input to the output, L1 regularization is applied. It penalizes for high absolute values of neurons' weights. Thus, it tries to determine inactive, sparse connections between neurons with assigned weights close to zero.

To incorporate temporal relationships of motion time series, subsequence anomalies are detected. It is realized by processing by the autoencoders in every detection, fixed-length segments of motion sequences. Moreover, for greater noise resistance, a kind of data augmentation is carried out. During the training stage, input data are modified by a random variable taken from the zero-mean Gaussian distribution with different standard deviations.

4 Dataset

The acquisition took place in the Human Dynamics and Multimodal Interaction Laboratory of the Polish-Japanese Academy of Information Technology. It is equipped with the Computer Assisted Rehabilitation ENvironment Extended system (CAREN Extended) manufactured by the Motek Company. It integrates

ICCS Camera Ready Version 2023
To cite this paper please use the final published version:
DOI: 10.1007/978-3-031-36021-3_59

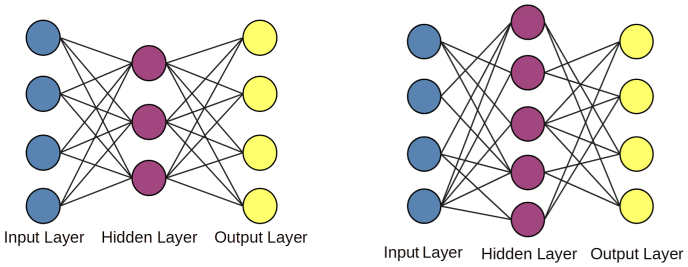

(a) Dense low-dimensional (b) Sparse high-dimensional

Fig. 2. The concept of the selected autoencoder architectures.

a 3D motion capture registration, dual-belt treadmill with 6 degrees of freedom (DoF) motion base and adaptive speed in the range $(0\frac{m}{s}, 15\frac{m}{s})$, ground reaction forces (GRF) and wireless electromyography (EMG) measurements, as well as immersive virtual/augmented reality environment with panoramic video and surround 5.1 audio subsystems. The laboratory is presented in Fig. 3. In the perspective (a) and front (b) views, the treadmill with the registered participant and curved screen are visible. In the bottom view (c), the construction with 6 DoF located below the motion base is shown.

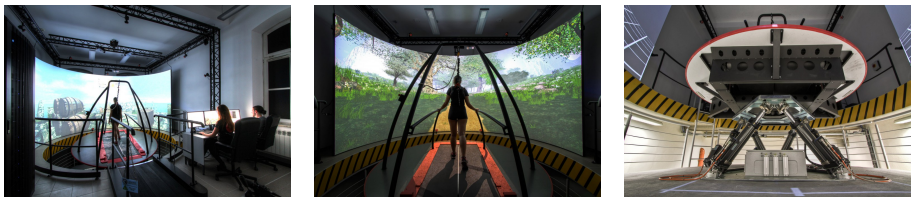

(a) Perspective view (b) Front view (c) Bottom view

Fig. 3. Human Dynamics and Multimodal Interaction Laboratory of the Polish-Japanese Academy of Information Technology.

The motion capture camera setup and applied skeleton model are visualized in Fig. 4. However, in the experiments, only segments followed by hip, knee, ankle, and wrist joints are taken into account. They are described by angles triplets expressed in the notation representing flexion/extension, adduction/abduction, and internal/external rotations in sagittal (lateral), frontal (coronal), and transverse planes. It means that body is divided into left/right, anterior/posterior (front/back), and superior/inferior (upper/lower) parts, respectively. There is only one exception – knee joints with single DoF have only a flexion angle. Thus, in total, the pose space is 20-dimensional.

ICCS Camera Ready Version 2023
To cite this paper please use the final published version:
DOI: 10.1007/978-3-031-36021-3_59

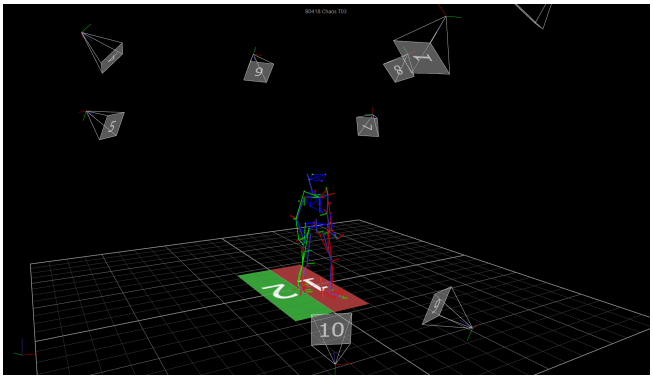

Fig. 4. Mocap camera setup and skeleton model.

To observe gait anomalies, three registration scenarios are proposed. They are located in the virtual reality of a forest, as visualized in Fig. 5. The first one is normal walking without any perturbations and provides anomaly-free data used in the training stage. The second one is related to video stimuli appearing in random time instants. There is a deer crossing the walking path, a simulation of the temporary darkness – the screen is off for one second – and a simulation of dizziness by floating visualization on the screen. In the last scenario, audio disturbances are included. The sounds of the horn, gunshot, and animal roar are generated.

Twelve participants were involved in the registration experiment. Every scenario was repeated three times, the duration of the recordings was approximately one minute, and the frequency of the acquisition was 100Hz. Time instants of the stimuli are exported, and they denote possible anomaly occurrences. Finally, on the basis of video recordings, manual labeling of the data was carried out to identify ultimate anomalies detected in the testing stage.

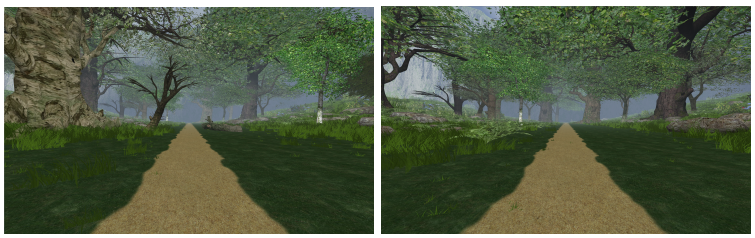

Fig. 5. Prepared virtual forest.

ICCS Camera Ready Version 2023
To cite this paper please use the final published version:
DOI: 10.1007/978-3-031-36021-3_59

5 Results

For labeled recordings of the scenarios with video and audio stimuli, anomaly detection is carried out by autoencoders trained using the data of the first scenario. On the basis of comparison with ground truth detections, true (TP) and false positives (FP) – numbers of properly and improperly recognized anomalies – as well as true (TN) and false (FN) negatives – the numbers of correctly determined normal instances and unidentified anomalies – are calculated. They are normalized through dividing by the total number of positives and negatives, respectively:

$$TPR = \frac{TP}{TP + FN} \tag{3}$$

$$FPR = \frac{FP}{FP + TN} \tag{4}$$

The balance between TPR and FPR is controlled by applying a threshold for the reconstruction error from equation (2). Thus, the curve called Receiver Operating Characteristic (ROC) representing the relationship between TPR and FPR values can be prepared. The area under this curve (ROC-AUC) is a measure of the detection performance.

However, in the faced anomaly identification challenge, the number of true negatives usually is much greater than true positives, which may have an influence on the ROC-AUC value. Therefore another measure is used in our evaluation protocol. It is based on precision and recall, which are true positives normalized by the total number of all positive identifications and all ground truth anomalies, respectively:

$$precision = \frac{TP}{TP + FP} \tag{5}$$

The recall is literally a true positive rate TPR. Once again, the balance between *precision* and *recall* is controlled by the threshold of the reconstruction error. It allows for determining precision for uniformly distributed recall values and calculating the average of them. This is, in fact, the area under the precision-recall curve and it is called average precision (AP). Moreover, to obtain a monotonic dependency, smoothing is carried out in such a way that every precision value is substituted by the maximum calculated for recalls equal to or greater than the current one.

The obtained results for dense low-dimensional and sparse high-dimensional autoencoders are depicted in Table 1 and Table 2, respectively. The lengths of the processed segments SL expressed by a number of time instants are 50 and 100. It means that half- and one-second subsequences are analyzed, which approximately correspond to half of and complete gait cycle with a single and double step performed. The number of inputs and outputs of the neural network is a product of SL and the dimensionality of pose space, which is 20. The angles are stored in degree scale, which means that injected Gaussian noises with standard deviations – 0.05, 0.1, 0.3, 0.5, 0.7 – are insignificant. The achieved AP and

ICCS Camera Ready Version 2023
To cite this paper please use the final published version:
DOI: 10.1007/978-3-031-36021-3_59

ROC-AUC values for the vast majority of cases are higher than 0.4 and 0.65, respectively. The best performance with AP = 0.462 and ROC-AUC = 0.708 is obtained by sparse autoencoder analyzing the one-second subsequences and having 3000 neurons of the hidden layer. For the considered variants, some general observations can be made: (i) slightly better precision of anomaly detection is achieved by high-dimensional sparse autoencoders and longer subsequences containing 100-time instants, (ii) there is an impact of injected noise on the effectiveness of the training process, but it differs depending on the autoencoder variant, (iii) both taken quality measures – AP and ROC-AUC – are partially correlated.

Table 1. Detection performances – AP and ROC-AUC (denoted as R-AUC) measures – of dense low-dimensional autoencoder with different standard deviations of injected Gaussian noise, number of neurons of the hidden layer D and length of the processed segments SL.

Noise		0.05		0.1		0.3		0.5		0.7	
D	SL	AP	R-AUC	AP	R-AUC	AP	R-AUC	AP	R-AUC	AP	R-AUC
25	50	0.394	0.660	0.405	0.667	0.390	0.654	0.373	0.649	0.343	0.621
50	50	0.408	0.667	0.406	0.667	0.402	0.668	0.382	0.651	0.371	0.646
100	50	0.405	0.677	0.424	0.679	0.405	0.678	0.403	0.666	0.393	0.662
200	50	0.436	0.683	0.428	0.679	0.415	0.672	0.402	0.670	0.393	0.658
400	50	0.423	0.672	0.434	0.682	0.441	0.693	0.430	0.683	0.408	0.675
50	100	0.414	0.677	0.412	0.672	0.416	0.674	0.389	0.678	0.380	0.634
100	100	0.419	0.678	0.436	0.694	0.423	0.679	0.398	0.662	0.393	0.650
200	100	0.430	0.683	0.432	0.693	0.424	0.680	0.430	0.686	0.384	0.646
400	100	0.438	0.688	0.428	0.681	0.442	0.694	0.439	0.686	0.410	0.672

Table 2. Detection performances – AP and ROC-AUC (denoted as R-AUC) measures – of sparse high-dimensional autoencoder with different standard deviations of injected Gaussian noise, number of neurons of the hidden layer D and length of the processed segments SL.

Noise		0.05		0.1		0.3		0.5		0.7	
D	SL	AP	R-AUC	AP	R-AUC	AP	R-AUC	AP	R-AUC	AP	R-AUC
1500	50	0.448	0.703	0.433	0.683	0.443	0.703	0.446	0.697	0.352	0.619
3000	100	0.462	0.708	0.461	0.704	0.417	0.673	0.445	0.700	0.432	0.699
5000	100	0.458	0.706	0.426	0.684	0.412	0.670	0.445	0.692	0.393	0.650
1250	50	0.423	0.670	0.447	0.691	0.413	0.675	0.344	0.617	0.327	0.592
2500	50	0.446	0.690	0.447	0.694	0.439	0.682	0.448	0.703	0.415	0.670
3500	50	0.455	0.691	0.445	0.692	0.434	0.687	0.439	0.700	0.437	0.688

The obtained results are at least promising and substantially better than random detection. They differ for successive participants as presented in Table 3

ICCS Camera Ready Version 2023
To cite this paper please use the final published version:
DOI: 10.1007/978-3-031-36021-3_59

Table 3. Best results – AP and ROC-AUC – obtained by the successive participants for sparse high-dimensional autoencoder ($D = 3000$, $SL = 100$).

Participant	AP	ROC-AUC	Percent of anomalies
1	0.578	0.833	0.082
2	0.541	0.750	0.167
3	0.227	0.695	0.109
4	0.636	0.761	0.204
5	0.396	0.619	0.201
6	0.377	0.646	0.113
7	0.223	0.615	0.113
8	0.454	0.690	0.135
9	0.305	0.709	0.113
10	0.848	0.828	0.383
11	0.739	0.816	0.257
12	0.216	0.531	0.187

– for some of them, anomalies are recognized pretty efficiently and for others, poorly. The balance between TPR and FPR as well as between precision and recall can be controlled by applying different threshold values for the reconstruction error. The example relationships for the best sparse autoencoder and successive participants are visualized in Fig. 6 and Fig. 7.

6 Summary and conclusions

The denoising dense low-dimensional and sparse high-dimensional autoencoders are applied in the anomaly detection of gait motion capture data. Due to the low number of samples of the training set, architectures containing only a single hidden layer are investigated. Obtained preliminary results with AP = 0.462 and ROC-AUC = 0.708 measures are certainly promising and prove that process of efficient gait anomaly identification is feasible.

The faced problem of abnormality detection of motion capture data is pretty challenging. The mocap sequences are described by highly multivariate time series, their anomalies may occur quite differently and depend on individual inclinations. What is more, the pose parameters are correlated and gait is performed in a chaotic way [19].

There are numerous possible improvements to investigate in future research. More exhaustive experiments related to neural network architectures and training parameters can be conducted. Moreover, instead of the angles representing segments' orientation in sagittal, frontal and transverse planes, Euler angles with the joint rotation or 3D position of the markers attached to the human body may be taken. The feature selection in the pose space or downsampling in the time domain reduces the number of trainable parameters of the autoencoder, which also may be advantageous. Ultimately, there are plenty of other techniques successfully applied for anomaly detection of similar data. Particularly approaches

ICCS Camera Ready Version 2023
To cite this paper please use the final published version:
DOI: 10.1007/978-3-031-36021-3_59

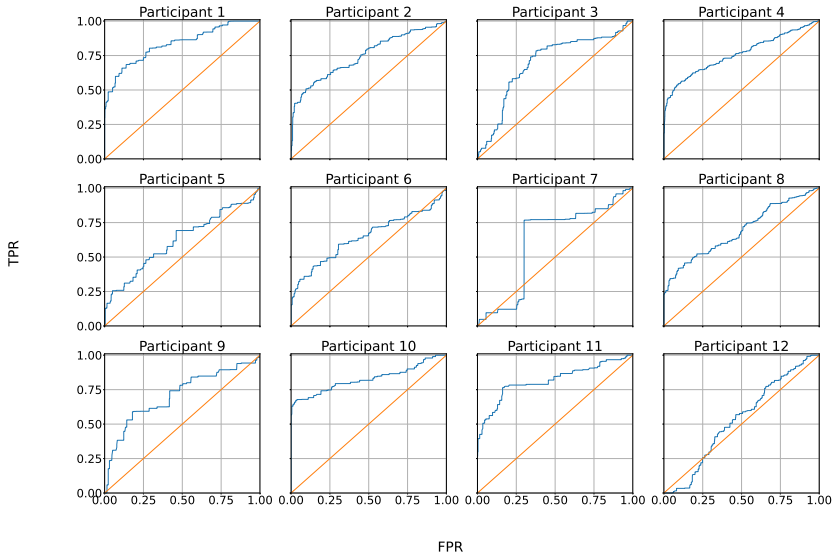

Fig. 6. Receiver Operating Characteristic (ROC) curves (sparse high dimensional autoencoder: $D = 3000$, $SL = 100$, noise std $= 0.05$) for subsequent participants. The blue and red colors correspond to the autoencoder and random guess classifier results, respectively.

predicting actual state on the basis of preceding time instants and LSTM networks [11] seem to be reasonable. In addition, it is planned to enlarge the dataset not only with measurements of new participants but also with extra scenarios. The effect of the stimuli will be intensified by their simultaneous occurrence, and new stimuli will be used.

Ethics statement

During the acquisition process, a non-invasive Vicon motion capture system was used. The measurements took place in the Human Dynamics and Multimodal Interaction Laboratory of the Polish-Japanese Academy of Information Technology and were assisted by the certified staff. The registration protocol contains normal gait and it is consistent with the Declaration of Helsinki. All the volunteers participating in the experiments were informed about the rules of acquisition and agreed to use their collected data for research purposes.

ICCS Camera Ready Version 2023
To cite this paper please use the final published version:
DOI: 10.1007/978-3-031-36021-3_59

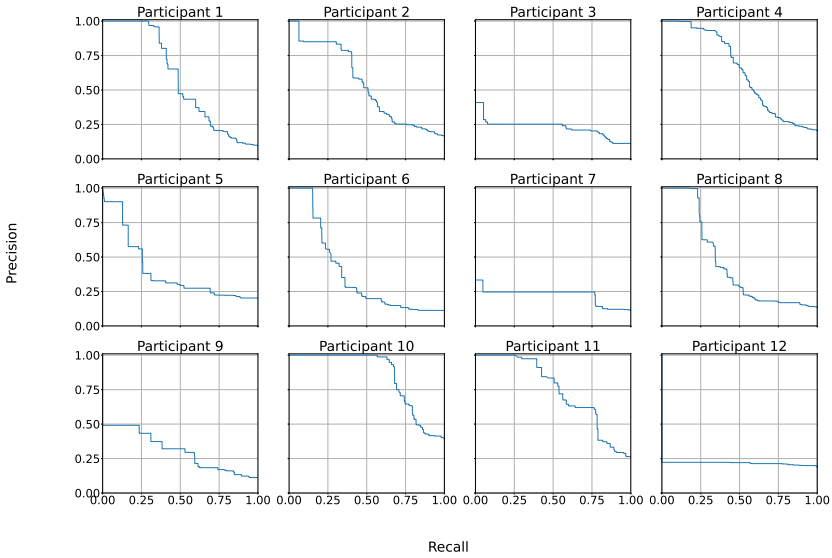

Fig. 7. Precision-recall curves (sparse high dimensional autoencoder: $D = 3000$, $SL = 100$, noise std $= 0.05$) for subsequent participants.

Acknowledgments

This work was supported by the Department of Computer Graphics, Vision, and Digital Systems, under the statue research project (Rau6, 2023), Silesian University of Technology (Gliwice, Poland).

References

1. An, J., Cho, S.: Variational autoencoder based anomaly detection using reconstruction probability. Special lecture on IE **2**(1), 1–18 (2015)
2. Barnachon, M., Bouakaz, S., Boufama, B., Guillou, E.: Ongoing human action recognition with motion capture. Pattern Recognition **47**(1), 238–247 (2014)
3. Basu, S., Meckesheimer, M.: Automatic outlier detection for time series: an application to sensor data. Knowledge and Information Systems **11**, 137–154 (2007)
4. Benkabou, S.E., Benabdeslem, K., Canitia, B.: Unsupervised outlier detection for time series by entropy and dynamic time warping. Knowledge and Information Systems **54**(2), 463–486 (2018)
5. Bente, G., Novotny, E., Roth, D., Al-Issa, A.: Beyond stereotypes: Analyzing gender and cultural differences in nonverbal rapport. Frontiers in Psychology **11**, 599703 (2020)
6. Błaszczyszyn, M., Szczęsna, A., Pawlyta, M., Marszałek, M., Karczmit, D.: Kinematic analysis of mae-geri kicks in beginner and advanced kyokushin karate athletes. International Journal of Environmental Research and Public Health **16**(17), 3155 (2019)

ICCS Camera Ready Version 2023
To cite this paper please use the final published version:
DOI: 10.1007/978-3-031-36021-3_59

7. Blázquez-García, A., Conde, A., Mori, U., Lozano, J.A.: A review on outlier/anomaly detection in time series data. ACM Computing Surveys (CSUR) **54**(3), 1–33 (2021)
8. Chandola, V., Banerjee, A., Kumar, V.: Anomaly detection: A survey. ACM computing surveys (CSUR) **41**(3), 1–58 (2009)
9. Dani, M.C., Jollois, F.X., Nadif, M., Freixo, C.: Adaptive threshold for anomaly detection using time series segmentation. In: Neural Information Processing: 22nd International Conference, ICONIP 2015, Istanbul, Turkey, November 9-12, 2015, Proceedings Part III 22. pp. 82–89. Springer (2015)
10. Gong, D., Liu, L., Le, V., Saha, B., Mansour, M.R., Venkatesh, S., Hengel, A.v.d.: Memorizing normality to detect anomaly: Memory-augmented deep autoencoder for unsupervised anomaly detection. In: Proceedings of the IEEE/CVF International Conference on Computer Vision. pp. 1705–1714 (2019)
11. Hundman, K., Constantinou, V., Laporte, C., Colwell, I., Soderstrom, T.: Detecting spacecraft anomalies using lstms and nonparametric dynamic thresholding. In: Proceedings of the 24th ACM SIGKDD International Conference on Knowledge Discovery & Data Mining. pp. 387–395 (2018)
12. Hyndman, R.J., Wang, E., Laptev, N.: Large-scale unusual time series detection. In: 2015 IEEE International Conference on Data Mining Workshop (ICDMW). pp. 1616–1619. IEEE (2015)
13. Keogh, E., Lin, J., Fu, A.: Hot sax: Efficiently finding the most unusual time series subsequence. In: Fifth IEEE International Conference on Data Mining (ICDM'05). pp. 8–pp. Ieee (2005)
14. Kieu, T., Yang, B., Jensen, C.S.: Outlier detection for multidimensional time series using deep neural networks. In: 2018 19th IEEE International Conference on Mobile Data Management (MDM). pp. 125–134. IEEE (2018)
15. Lara, J.A., Lizcano, D., Rampérez, V., Soriano, J.: A method for outlier detection based on cluster analysis and visual expert criteria. Expert Systems **37**(5), e12473 (2020)
16. Liparoti, M., Della Corte, M., Rucco, R., Sorrentino, P., Sparaco, M., Capuano, R., Minino, R., Lavorgna, L., Agosti, V., Sorrentino, G., et al.: Gait abnormalities in minimally disabled people with multiple sclerosis: A 3d-motion analysis study. Multiple Sclerosis and Related Disorders **29**, 100–107 (2019)
17. Munir, M., Siddiqui, S.A., Dengel, A., Ahmed, S.: Deepant: A deep learning approach for unsupervised anomaly detection in time series. IEEE Access **7**, 1991–2005 (2018)
18. Pang, G., Shen, C., Cao, L., Hengel, A.V.D.: Deep learning for anomaly detection: A review. ACM Computing Surveys (CSUR) **54**(2), 1–38 (2021)
19. Piórek, M., Josiński, H., Michalczuk, A., Świtoński, A., Szczęsna, A.: Quaternions and joint angles in an analysis of local stability of gait for different variants of walking speed and treadmill slope. Information Sciences **384**, 263–280 (2017)
20. Rebbapragada, U., Protopapas, P., Brodley, C.E., Alcock, C.: Finding anomalous periodic time series: An application to catalogs of periodic variable stars. arXiv preprint arXiv:0905.3428 (2009)
21. Reddy, A., Ordway-West, M., Lee, M., Dugan, M., Whitney, J., Kahana, R., Ford, B., Muedsam, J., Henslee, A., Rao, M.: Using gaussian mixture models to detect outliers in seasonal univariate network traffic. In: 2017 IEEE Security and Privacy Workshops (SPW). pp. 229–234. IEEE (2017)
22. Song, S., Zhang, A., Wang, J., Yu, P.S.: Screen: stream data cleaning under speed constraints. In: Proceedings of the 2015 ACM SIGMOD International Conference on Management of Data. pp. 827–841 (2015)

ICCS Camera Ready Version 2023
To cite this paper please use the final published version:
DOI: 10.1007/978-3-031-36021-3_59

23. Świtoński, A., Josiński, H., Wojciechowski, K.: Dynamic time warping in classification and selection of motion capture data. Multidimensional Systems and Signal Processing **30**, 1437–1468 (2019)
24. Zhang, A., Song, S., Wang, J.: Sequential data cleaning: A statistical approach. In: Proceedings of the 2016 International Conference on Management of Data. pp. 909–924 (2016)
25. Zhang, Y., Hamm, N.A., Meratnia, N., Stein, A., Van de Voort, M., Havinga, P.J.: Statistics-based outlier detection for wireless sensor networks. International Journal of Geographical Information Science **26**(8), 1373–1392 (2012)

ICCS Camera Ready Version 2023
To cite this paper please use the final published version:
DOI: 10.1007/978-3-031-36021-3_59